Jour. of the KGS, Vol. 21, No. 2. March 2005, pp. 67~84

Effects of Geosynthetic Reinforcement on Compaction of High Water Content Clay

토목섬유 보강이 고함수비 점성토의 다짐에 미치는 영향

Roh, Han-Sung[1] 노 한 성

요 지

본 연구는 포화된 연약 점성토에 대한 보강효과를 분석하기 위하여 롤러 다짐장비를 사용하여 수행하였다. 시료는 12시간 수침으로 포화 상태를 만들었으며, 철재 롤러로 평면변형율 상태에서 5cm 층두께로 4층의 다짐을 실시하였다. 보강효과를 분석하기 위하여 무보강 조건 및 부직포와 직포로 구성된 복합보강재를 사용한 보강조건으로 다짐 공시체를 제작하였다. 복합보강재의 배수효과와 인장 보강효과로 고함수비 점성토의 지지력을 증가시켜, 보강토에 대하여 큰 다짐하중을 가할 수 있게 되어 보다 큰 밀도를 효과적으로 얻을 수 있다. 또한 다짐작업시 보강재에 의해 연직재하 하중에 대한 전단저항 반력의 감소에 의해 다짐효율을 증가시킨다. 공시체 저면에서의 최대 연직응력은 다짐두께가 증가 할수록 감소하게 된다. 한편 보강재는 롤러의 연직하부의 지반강성을 증가시켜 응력집중현상이 발생한다. 이로인하여 공시체 저면에서 보다 높은 연직응력 수준을 유지하며 보다 효과적인 다짐특성을 제공하게 된다. 시험결과로부터 연약점성토의 효과적인 다짐을 위해서는 보강재가 필수적으로 요구된다고 할 수 있다.

Abstract

This research was conducted to evaluate the effectiveness of reinforcement for nearly saturated soft clay compaction. The effectiveness was investigated by roller compaction test using nearly saturated clay specimens. The nearly saturated condition was obtained by submerging clay in the water for 12 hours. High water content specimens were compacted in plane strain condition by a steel roller. A specimen was compacted by four 5 cm horizontal layers. Specimens were prepared for both reinforced and unreinforced cases to evaluate the effectiveness of reinforcement. Used reinforcement is a composite consisted of both woven and non-woven geotextile. The composite usually provides drainage and tensile reinforcement to high water-contented clay so that it increases bearing capacity. Therefore, large compaction load can be applied to reinforced clay and it achieves higher density effectively. The reinforcement also increases compaction efficiency because it reduces the ratio between shear and vertical forces during compaction process. The maximum vertical stress on the base of specimen usually decreased with higher compaction thickness. The reinforcement increases soil stiffness under the compaction roller and it initiates stress concentration. As a result, it maintains higher vertical stress level on the base of specimen that provides better compaction characteristics. Based on test results, it can be concluded that the reinforcement is essential to achieve effective compaction on soft clay.

Keywords : Effective compaction, Geosynthetic-reinforced saturated clay, Roller compaction test, Soil stiffness, Stress concentration

1 Professional Engineer, Project Development Division, Korea Highway Corporation (hsroh@freeway.co.kr)

1. Introduction

It is very difficult to achieve good strength and stiffness for high water-contented clayey soil through compaction. Hence, high water-contented clayey soil is not used for backfill soil of reinforced soil structures, including steel-reinforced soil retaining walls. However, newly invented Rigid facing Reinforced Retaining wall (RRR) allows clayey soil to be the backfill. This new retaining wall system was invented by the University of Tokyo and the Railway Technical Research Institute (RTRI) in Japan. They have conducted series of field tests to evaluate the feasibility of marginal soil as backfill (Nagano wall; Tatsuoka et al. 1997a, 2000).

A recent study proves that the high water-content clay can provide enough strength and stiffness to be used as backfill for important civil engineering structures(Roh and Tatsuoka, 2001). Applying tensile reinforcement with preloading and prestressing procedures only allows minimal deformation in the body of compacted high water-content clay. Although aforementioned study encourages the application of soft clay to backfill material, the workability problem is still remained in the construction field.

The present study investigates the effectiveness of a composite reinforcement on high water-contented clayey soil during compaction. This paper summarizes the laboratory test procedures, named roller compaction test, and results for reinforced saturated clay. For comparison purposes, unreinforced saturated clay was also tested by the same method. This paper also discusses engineering implications of research outcome. The research presented in this paper covers a part of the reinforcement technology of high-water content clay conducted at the University of Tokyo and the Railway Technical Research Institute (RTRI) in Japan (Tatsuoka et al. 1997a & b, Uchimura et al. 1997, 1999, 2000).

2. Study on Reinforced Clay

Jewell (1988) provided a rational understanding for the role of reinforcement in soft soil embankment. He suggested that the basal reinforcement resisted the soil pressure developed in the embankment and the lateral deformation in the foundation. It is a result of increased bearing capacity and stability by the reinforcement. Imanishi (2002) suggested a geogrid reinforcement for soft clay on the road construction. This method provides high bearing capacity for very soft clay without heavy machinery during the compaction. Based on these studies, it is anticipated that the bearing capacity of soft clay can be increased by the reinforcement. However, effects of reinforcement on the compaction efficiency were not evaluated systematically in previous studies.

A series of studies were performed to evaluate the feasibility of reinforced retaining wall with the clay backfill at the University of Tokyo and RTRI in Japan. This research was conducted with full-scale test embankments at Chiba, Japan and plane strain compression test in laboratory (Tatsuoka and Yamauchi 1988; Ling and Tatsuoka 1994; Tatsuoka et al. 1996, 1997a & b, 2000; Roh and Tatsuoka 2001). The Chiba test embankments were constructed with on-site high water-content volcanic-origin clay (so-called Kanto loam) for vertical walls. Tatsuoka and Yamauchi (1988) evaluated the effect of the wall facing stiffness and the vertical spacing of reinforcement on the behaviour of the walls of reinforced embankments by measuring the deformation of embankments.

According to Ling and Tatsuoka (1994), it is difficult to reinforce saturated soft clay under undrained conditions. A reinforced clay specimen exhibited a peak strength under drained conditions. It was much higher than that of the corresponding unreinforced clay specimen. It was particularly the case when the reinforced specimen was consolidated anisotropically at a ratio of the vertical to horizontal stresses σ'_v / σ'_h higher than the value for one-dimensional compression. Because some tensile strains were developed in reinforcement already during anisotropic consolidation stage. This result is consistent with the fact found in the nearly vertical walls of experimental clay embankment. They have been stable under drained conditions for a long period. Based on the experiences discussed above, the first prototype retaining wall was constructed to support a high-speed train parking yard with a high water-contented clay backfill (Tatsuoka et al. 1997a, 2000).

Another test embankment was constructed to evaluate the effectiveness of the preloading and prestressing procedures on the behaviour of geosynthetic-reinforced soil retaining walls (Tatsuoka et al. 1996, 1997a & b). This procedure has been proposed to increase the vertical stiffness of geosynthetic-reinforced soil. To make the deformation characteristic of reinforced soil be elastic, sufficiently large vertical preload is applied to it. To keep the high stiffness of reinforced soil, the preload is unloaded to a certain value which maintains high vertical pressure as prestress within reinforced soil (Fig. 1).

This test construction includes a few vertical walls. Types of backfill soil were Kanto loam clay (used for Chiba test embankment) and well-graded gravel. It was found that the clay backfill reinforced with a composite became very stiff against vertical load applied at the crest of backfill by vertically preloading in advance. The magnitude of creep deformation with vertical preloading is substantially smaller than that without preloading, if other test set-ups are identical. A series of drained tri-axial tests on the backfill clay also showed that the preloading procedure decreased the creep deformation substantially (Tatsuoka et al. 1996).

Based on these results, a 2.7 m-high prototype geogrid-reinforced gravel structure was constructed for the railroad bridge pier in September 1996 in the Fukuoka City (Tatsuoka et al. 1997a & b, Uchimura et al. 1997, 1999, 2000). The backfill was compacted well-graded crushed sandstone gravel with polymer geogrid reinforcement. The average vertical spacing was 15 cm between reinforcements.

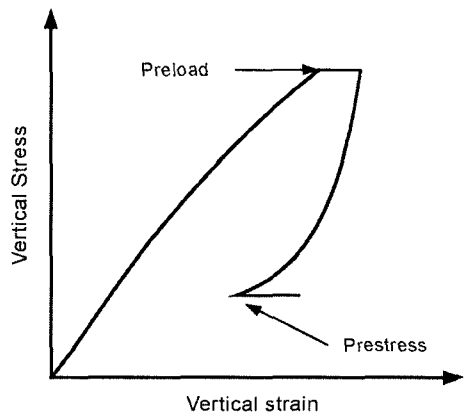

Fig. 1. Preload and prestress

The backfill was preloaded and prestressed until the half of the preload existed at the last stage of wall construction. The structure was in service since the beginning of August 1997. The pier showed very good performance since the construction.

Roh and Tatsuoka (2001) carried out plane strain compression test to evaluate the effects of the preloading and prestressing on the deformation characteristics of reinforced clay. They found that the effects of preloading and prestressing on the undrained stress-strain behaviour of geosynthetic-reinforced clay are basically similar to the drained behavior of sand and gravel. Based on this result, it can be said that high water-contented clay can be used as backfill material with tensile reinforcement.

In summary, the results from the full-scale field and laboratory tests indicated that high water-contented clay can be treated strong and stiff using tensile reinforcement with preloading and prestressing procedures. This feasibility is supported by the high performance of a prototype preloaded and prestressed geosynthetic-reinforced gravel pier. We found that the preloading and prestressing procedures improved the performance of clay in embankment. However, it is difficult to construct an embankment with very soft clay effectively. The main reason is that the very soft clay has low strength, low bearing capacity, and low trafficability. The present study was conducted to evaluate the effect of reinforcement on compaction by performing roller compaction test in laboratory.

3. Test Procedures

3.1 Apparatus and Test Specimens

Plane strain compaction apparatus

A roller compaction test system was designed to investigate the behaviour of reinforced soft clay during compaction (Fig. 2). Fig. 3 shows the systematic diagram of compaction mould in the test system. The nominal dimensions of specimen after compaction were 20 cm in height (H), 60 cm in length (L) (in the direction of the roller), and 40 cm in width (W) (in the direction of zero normal strain). The length of specimen was determined

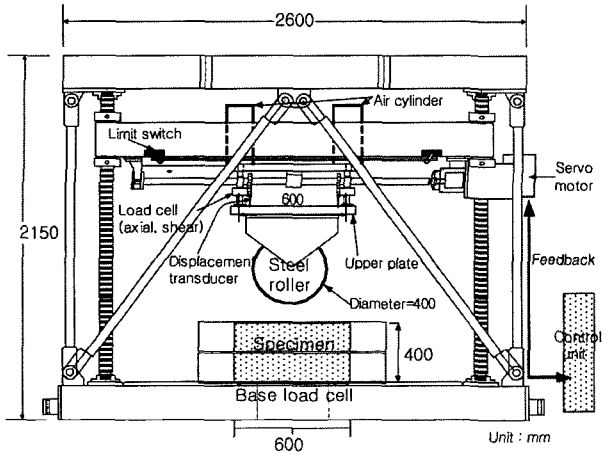

Fig. 2. Compaction machine

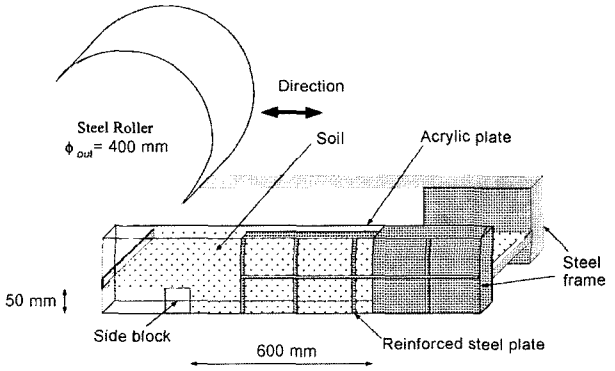

Fig. 3. Compaction mould

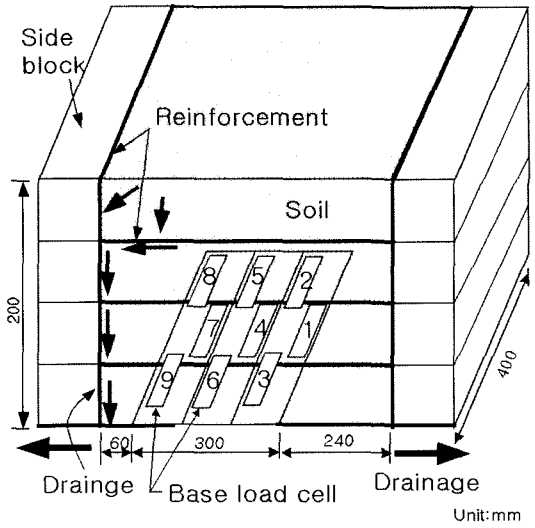

(a) Drainage paths

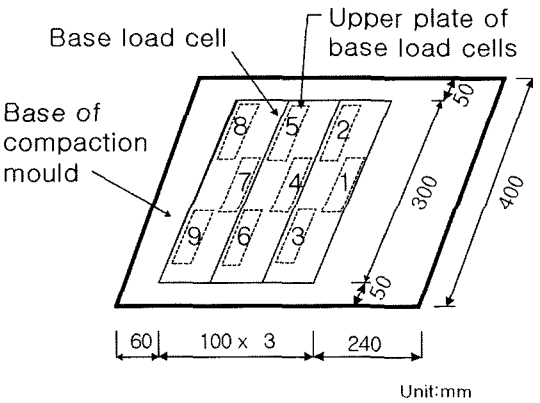

(b) Base load cells

Fig. 4. Drainage paths and base load cells

to be longer than the width in order to achieve higher reinforcing effects with long reinforcement.

Two sides of mould were made from acrylic plate with 3 cm thickness. The side plate allows us to see the behaviour of soil during the roller compaction test. Plane strain condition was achieved by steel frame of the mould. The smooth steel roller (ϕ=40 cm) applies the vertical load to the specimen using four air-cylinders attached intermediate deck. The roller was controlled by an analogue servo-motor and gear system to achieve constant horizontal speed (MPF005, Huji Electronic Co., Fig. 2). All tests were performed with the automated force control and maintained constant speed by closed-loop system.

A specimen was compacted by four 5 cm horizontal layers. A reinforced specimen contains reinforcement layers placed horizontally between layers. Fig. 4 shows drainage paths through a reinforced specimen. The composite reinforcement provides drainage paths in specimen. The outlets for the water through the specimen are the two sides of bottom specimen during compaction work.

Measurement components

The measured force components are: the applied vertical force P, the shear force S_F, the reaction vertical force at the base R_V, and the reaction shear force at the base R_H. The measured displacement components are the horizontal displacement of roller D_H and the vertical displacement of roller D_V. The settlement during compaction equals to D_V. The displacement D_H and D_V were defined zero at the beginning of compaction (immediately after roller touches to soil surface). The local strains of woven geotextile were measured to verify the tensile reinforcing effect of reinforcement for test Nos. 4 and 5 (Fig. 5).

The values of P and S_F reported in this paper are the sum of the four two-axial load cells measured at the upper

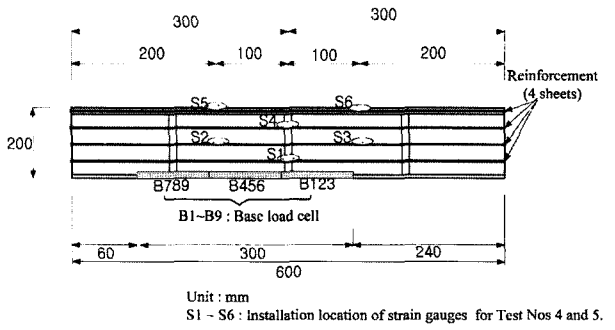

Fig. 5. Location of strain measurement on the reinforcement

side of roller. The values of R_V and R_H are the sum of the three load cells measured at the base. They equal to the resultant force on the area of 10 cm in width and 30 cm in length. Note that there are three sets of base load cells, so the total number of load cell is nine at the base (Fig. 4 (b)).

Fig. 6 shows the total applied vertical force P and total shear load acting on the roller S_F obtained from a typical compaction test on a reinforced specimen (Test No. 3, see Table 2 for the test numbers). The error between the measured and the target of P was in the range of ± 20%. It takes about three seconds for the feedback control. This infers that the roller speed is relatively high compared to quasi-static control system. The applied shear load S_F was displayed like a loop. That means the moving direction of roller was changed three times during compaction for each layer. It can be noted that a passive resistance was increasing toward each side due to the increasing volume of soil in resistance (Fig. 6 (b)).

3.2 Test Materials

The clay used in the laboratory test was retrieved from the reinforced clay backfill of the full-scale experimental embankments constructed at Chiba in Japan (Tatsuoka and Yamauchi 1988; Tatsuoka et al. 1991, 1993, 1997a, 2000). The sample was made air-dried, mechanically crushed and sieved to a diameter of less than 1 mm (Roh and Tatsuoka 2001). As listed in Table 1, the clay became less plastic by these treatments. Figs. 7 (a) and 7 (b) show the grain size distribution and compaction curve of the test clay after treatments.

The composite used in the test is made of 0.5 mm-thick polyester woven geotextile layer sandwiched between two 100% polypropylene non-woven geotextile layers (Fig. 8 (a)). The unit area mass of the woven and non-woven geotextiles was 460 g/m^2 and 310 g/m^2 each. The initial stiffness and rupture strength of the composite were 2,300 MN/m and 212 MN/m, respectively. This composite is identical to the one used in the previous tests (Roh and

Table 1. Physical properties of the tested clay before and after sieving

Properties	Before sieving (in the field)	After sieving (used in the study)
Specific gravity	2.899	2.81
Natural water content (%)	80~100	–
Liquid limit (%)	168.3	76.2
Plastic limit (%)	115.0	55.8
Plastic index	53.4	20.4

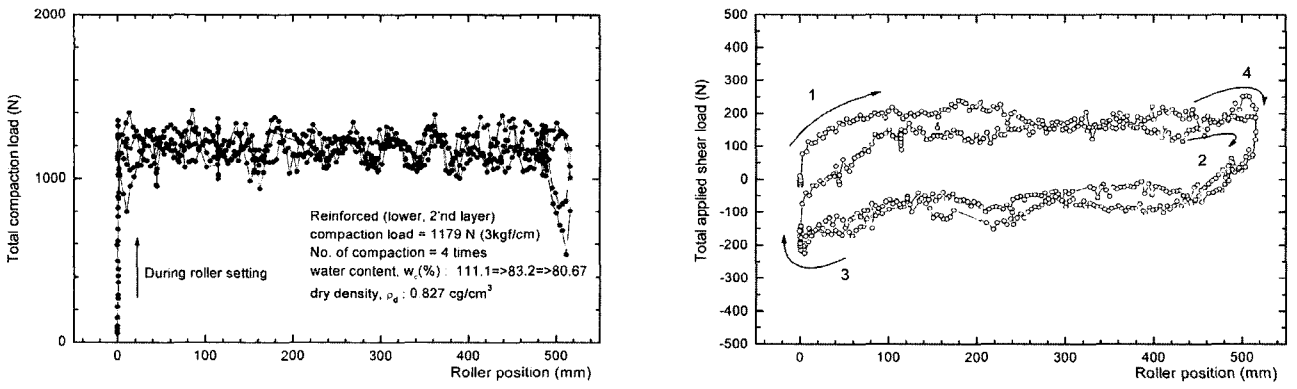

(a) Total applied vertical force

(b) Total applied shear load

Fig. 6. Typical results of total applied forces (Test No. 3)

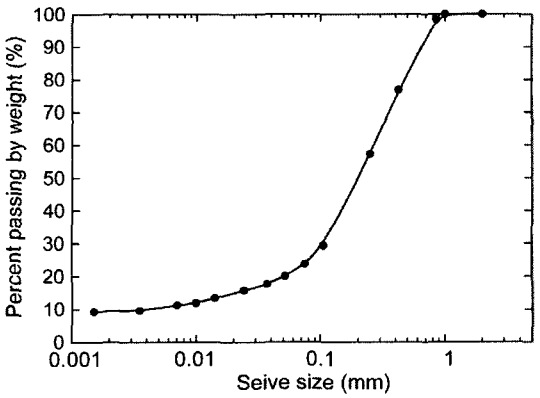

(a) Grain size distribution

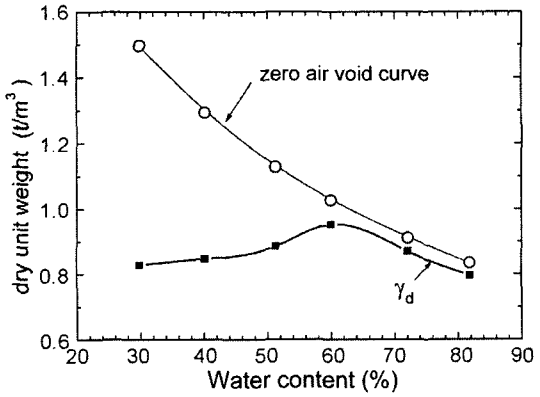

(b) Compaction curve

Fig. 7. Properties of the test clay

Tatsuoka, 2001). Fig. 8 (b) shows the compression properties of the composite and the spun-bond non-woven geotextile. Fig. 8 (c) presents the strength properties of the composite obtained from a tensile test using a 30-cm wide specimen performed at the axial strain rate of 2%/min (Ling et al. 1992).

3.3 Specimen Preparation for Compaction Test

The major part of embankment is usually located above ground water level in the field. Therefore embankment material may not be fully saturated (e.g., Tatsuoka and Yamauchi 1988). Due to the percolation of rainwater, the embankment material may become nearly saturated. It was decided to evaluate the effectiveness of reinforcement on compaction under such extreme field conditions (i.e., saturated conditions). The bearing capacity and trafficability of soil would become lowest in this condition. The clay was submerged in the water to get the saturated condition

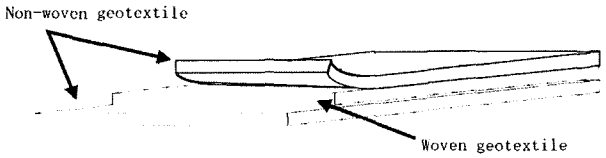

(a) Schematic diagram showing the reinforcement material (composite of non-woven and woven geotextiles)

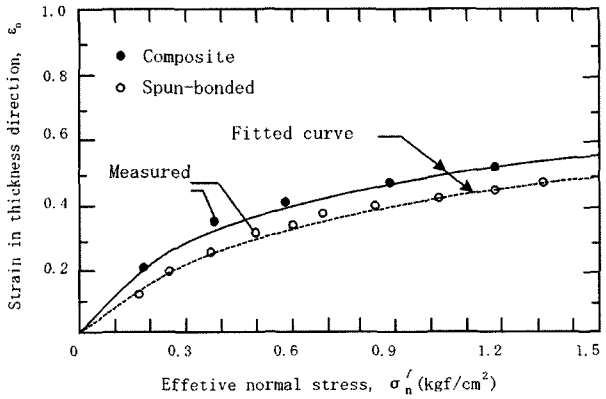

(b) Compression test result

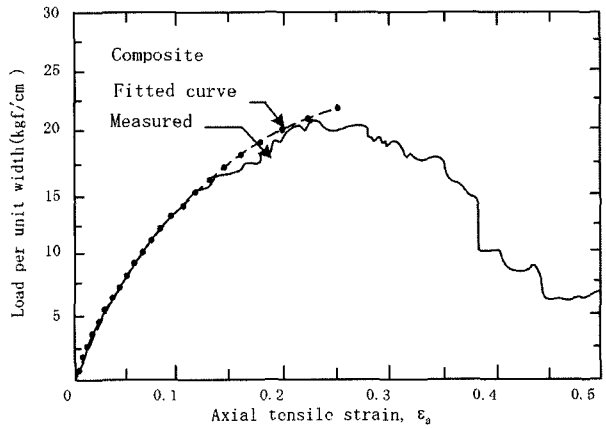

(c) Results from tensile test of the composite

Fig. 8. Composite reinforcement (Ling et al. 1992)

for more than 12 hours. A saturation ratio S_r of sample is about 100% when placing a layer.

3.4 Loading Control of Compaction

Each specimen was made with the roller compaction method using feedback control. The vertical load was controlled by two sets of two air cylinders (Fig. 2). The pressure of four air cylinders was regulated by EP transducers. The vertical load increased from zero to the target value with levelling of the upper plate above roller after the clay was set in the mould. Each layer was compacted four times. The water content and density were measured

just after compaction. The applied vertical load was adjusted by using EP transducers if the difference between applied and target value of compaction load was greater than 100N. The upper plate above roller could be inclined due to the unbalanced soil reaction between front and back of roller. It means that the roller speed would not constant. The required pressures of air cylinders were computed to maintain constant speed of roller, considering both compaction load and level of upper plate above roller.

The target compaction loads were 393N, 1177N, and 2358N (1, 3, and 6 kg/cm in wheel line load respectively) in this study. The roller speed was selected as 1.3 mm/sec to obtain enough data and to avoid speed effect of roller.

Fig. 9 shows the measured total compaction loads obtained from all tests (listed in Table 2). Despite variance of data, it can be said that the error ratio of the measured to a target value of total compaction load decreases with increasing the compaction load. It may also be noted from test No. 5 in Fig. 8 that the bearing capacity of soft clay before compacted is smaller than applied compaction load. The compaction load becomes noticeably smaller than the target value when roller moving stopped.

When roller position was close to each boundary, applied vertical load was unstable due to the discontinuity of stiffness between soft clay and steel block at side (see Fig. 3). However, it can be said that compaction work was well controlled in the center of a specimen where important measurement was measured.

Figs. 10 shows the relationships between the stress ratio of shear force versus vertical force (S_a=S_F/P) and roller position for all tests. The shear force S_F is a reaction that is

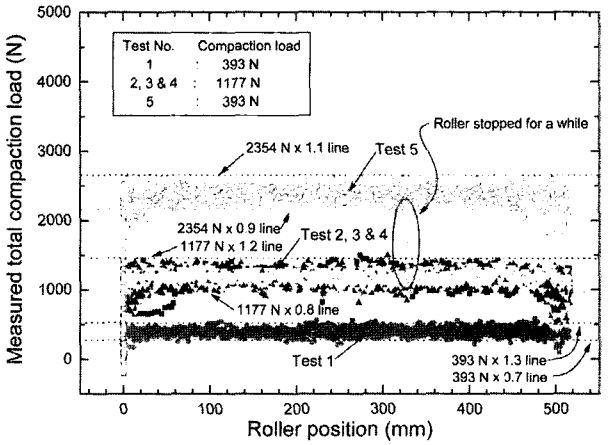

Fig. 9. Measured total compaction loads relevant to the roller position

Table 2. List of the tests performed in the present study

Test No.	Reinforcement	Compacton load : kgf/cm (Total Load : N)	Layer No.	Variation of soil properties (Before compaction → After compaction	
				Water content (%)	Unit dry weight (t/m^3)
1	Unreinforcement	1 (393)	1	95.3 → 78.6	– → 0.816
			2	99.0 → 91.1	
2	Unreinforcement	3 (1177)	1	94.1 → 77.7	0.746 → 0.832
			2	97.5 → 75.4	→ 0.838
			3	91.8 → 74.4	→ 0.842
			4	93.3 → 86.7	→ 0.807
3	Reinforcement (Under)	3 (1177)	1	91.3[1] → 83.3	0.740 → 0.794
			2	111.1 → 80.7	→ 0.827
			3	105.0 → 79.7	→ 0.853
			4	108.7 → 83.3	→ 0.821
4	Reinforcement (Under)	3 (1177)	1	99.9 → 81.3	0.736 → 0.804
			2	99.9 → 79.1	→ 0.821
			3	98.3 → 74.5	→ 0.845
			4	101.5 → 77.6	→ 0.831
5	Reinforcement (Under)	6 (2358)	1	94.1 → 68.5	0.777 → 0.890
			2	92.7 → 64.3	0.745 → 0.922
			3	91.0 → 62.8	0.752 → 0.949
			4	89.4 → 66.8	0.783 → 0.929

caused by horizontal passive soil pressure on roller. A large value of S_a indicates a large shear force initiated by large soil settlement. Relatively large value of S_a is obtained for unrienforced case rather than reinforced case (compare Figs. 10 (b), 10 (c), and 10 (d)) and for increased compaction load (refer Figs. 10 (a) and 10 (b), Figs. 10 (d) and 10 (e)). The smaller shear force is developed with decreased settlement of soil by reinforcement.

3.5 Test Programme

The effects of the following factors were evaluated by performing the tests listed in Table 2:

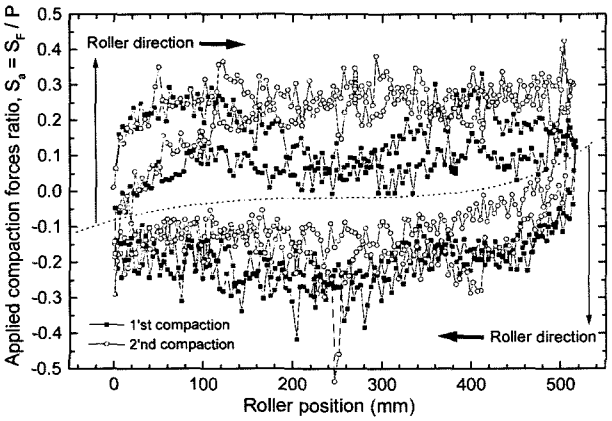

(a) Unreinforced (compaction load : 393N)

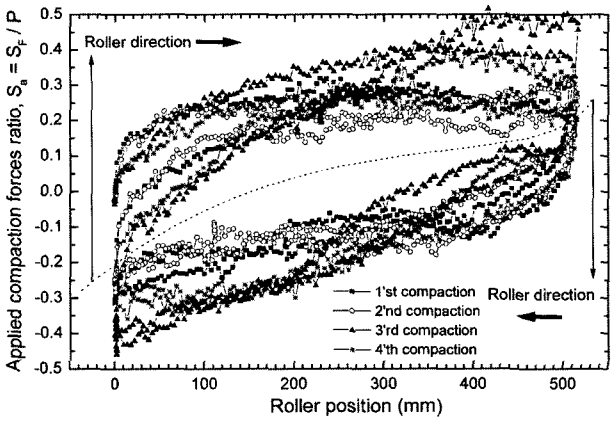

(b) Unreinforced (compaction load : 1177N)

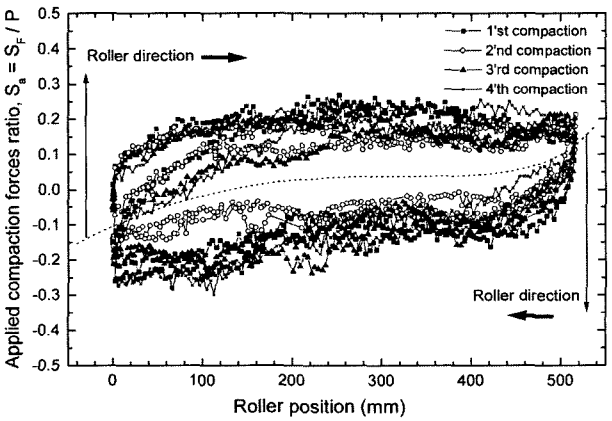

(c) Reinforced (lower), compaction load : 1177N

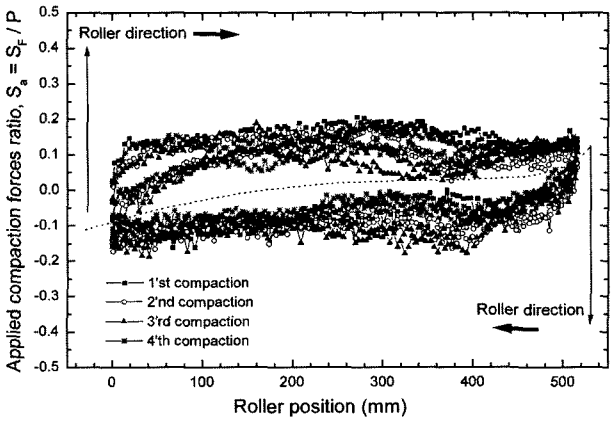

(d) Reinforced (upper), compaction load : 1177N

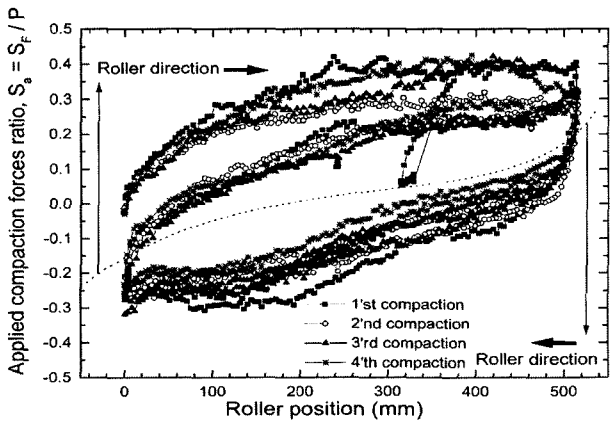

(e) Reinforced (upper), compaction load : 2358N

Fig. 10. Applied compaction forces ratio, Sa (=total shear force/total vertical load) relevant to the roller position

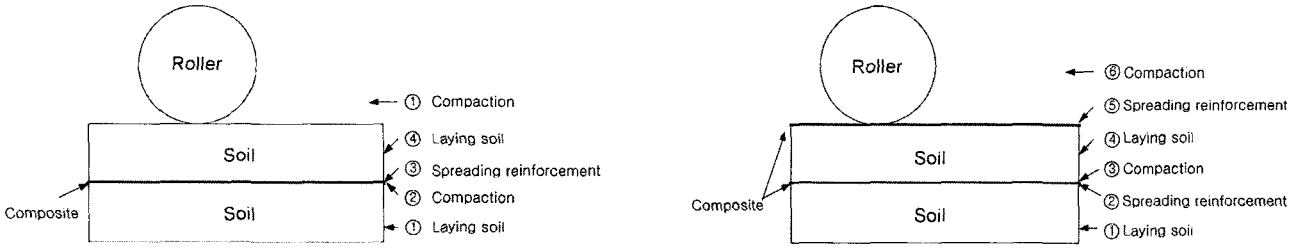

(a) Reinforced under placing layer (b) Reinforced over placing layer

Fig. 11. Compaction methods with reinforcement

(1) *reinforcement*, evaluated by comparing compaction behaviors of unreinforced and reinforced specimens;
(2) *compaction load*, estimated by comparing compaction behaviors and soil properties of specimens for different compaction load.
(3) *reinforcing method*, evaluated by comparing compaction behaviors of reinforced specimens for two reinforcing methods (Fig. 11). One is spreading reinforcement below compacted layer and another is layering reinforcement on compacted layer surface.

4. Test Results and Discussions

4.1 Settlement

The settlement ratio S_R is defined as the ratio of settlement value S_m to the height of laying soil layer H_o (Fig. 12). The magnitude of S_m is the total vertical deformation. It is the summation of compacted layer thickness and vertical displacement caused from pushed soil by roller. For experimental convenience, over compaction is defined when S_m equals to the height of each compacted layer.

Fig. 13 shows the relationship between settlement ratio of roller S_R and the number of roller passing for tests. From the observation of tests, followings were found:

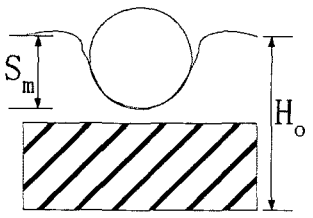

Fig. 12. Definition of settlement ratio, S_R

(1) The settlement S_m increased with more number of compaction in a layer. S_m also increased with higher compaction load for the unreinforced and reinforced specimens respectively (Test No.1 and 2: Test No. 4 and 5).
(2) The overall $S_R \sim N$ relationships were linear with relatively soft behavior due to the effects of initial high water content on clay.
(3) The noticeable effects of reinforcement can be seen at the last compaction layer. It means that tensile-reinforcing effect of reinforcement was developed by compaction. The reinforcement increased the effective confining pressure in soil element and bearing capacity of clay adjacent roller. Therefore, it decreased the amount of pushed-out soil. This trend can be noted clearly in Fig. 26 and Fig. 27. The tensile strain of reinforcement was very large value beneath the roller during compaction. The result suggested that the reinforcement allows larger compaction load to the soft clay specimen (Test No. 2 and 5).
(4) However, the large amount of settlement was inevitable in this study due to the short length of reinforcement in the specimens.

4.2 Dry Unit Density and Water Content

Fig. 14 shows the relationship between dry unit density γ_d and the water content w from ω compaction tests. It can be seen that the overall γ_d - ω relationships are following zero air void ratio curve. Note that the largest compaction load applied was obtained from Test No. 5. It has the greatest dry unit density and the smallest water

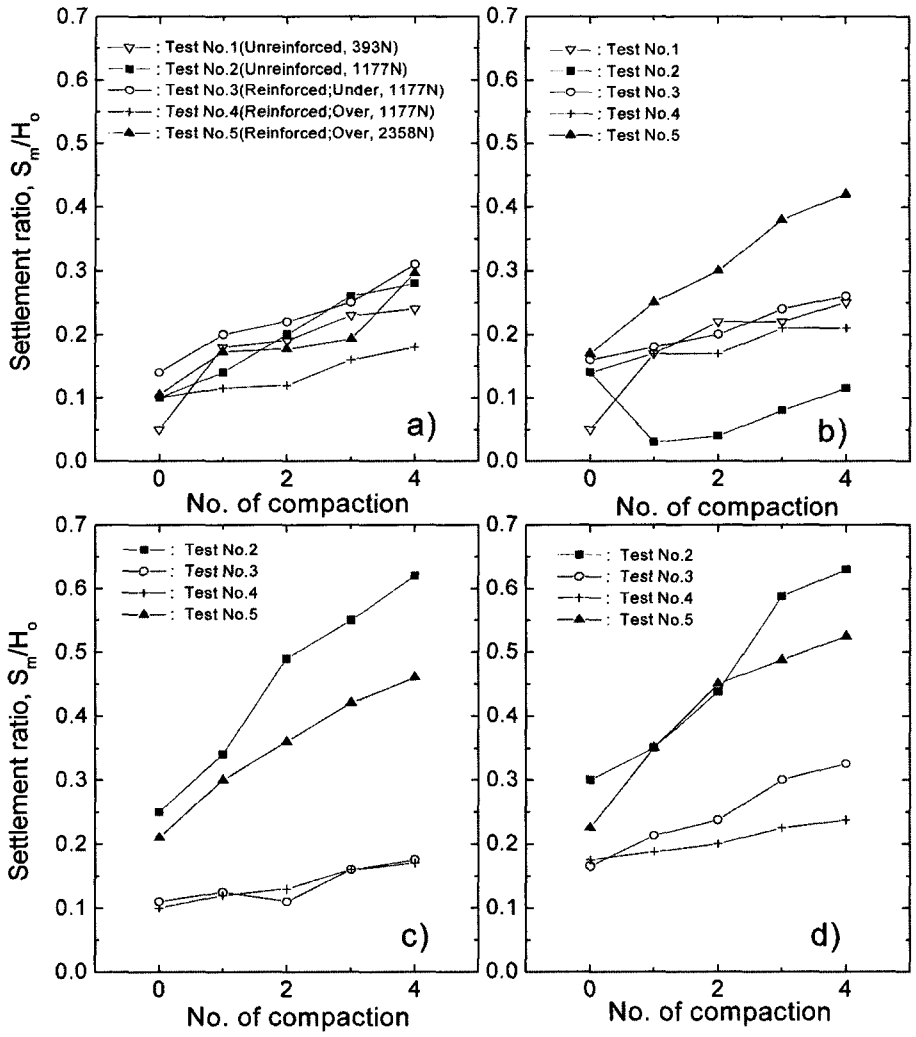

Fig. 13. Relationship between settlement ratio of roller S_R (=settlement after compaction / height of placing layer) and the number of roller passing N for all tests; a) 1st ; layer b) 2nd ; layer c) 3rd layer; and d) 4th layer

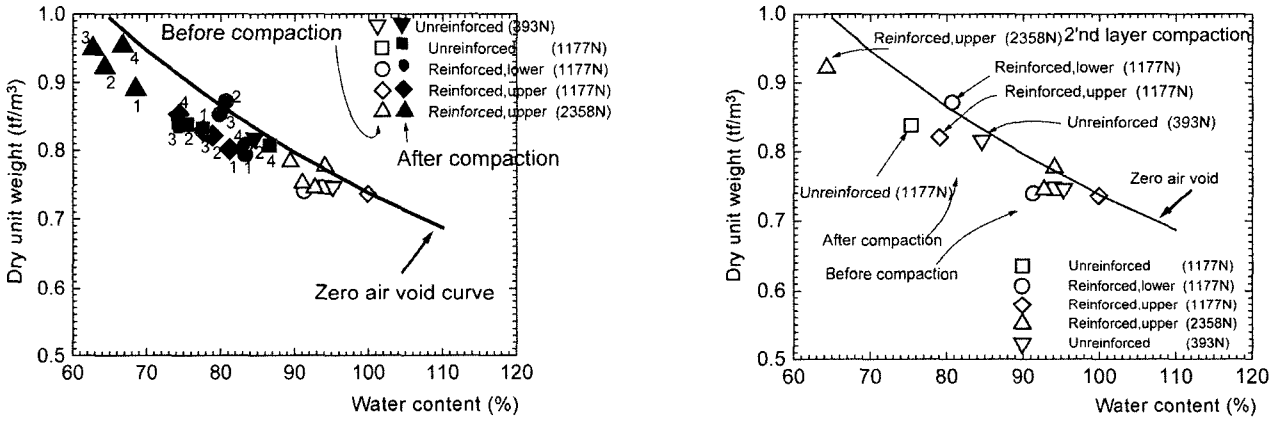

(a) All layers

(b) Last compaction layer of all test

Fig. 14. Relationship between dry unit weight and water content

content by compaction. It can be concluded that the compaction efficiency was increased by reinforcement.

4.3 Stress at the Base

It is well known that Boussinesq considered a point

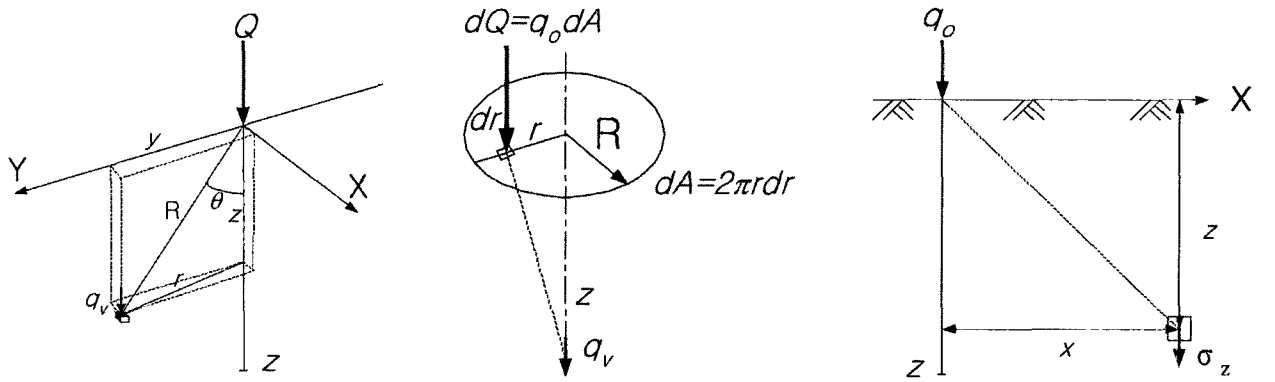

(a) Below the surface acted on by point load Q in 3D (b) below the center of a circular area acted on by intensity of pressure q_0 (c) below the surface acted on by point load q_0 in 2D

Fig. 15. Pressure at a point of depth z

load on the surface of an infinitely large homogeneous, isotropic, weightless, and elastic half-space to obtain equations 1 and 2.

$$q_r = \frac{3Q}{2\pi z^2}\cos^5\theta \tag{1}$$

$$q_r = \frac{3Qz^3}{2\pi R^5} = \frac{3Q}{2\pi z^2}\frac{1}{[1+(r/z)^2]^{5/2}} = \frac{Q}{z^2}A_b \tag{2}$$

Where, symbols are identified in Figs. 15 (a) and 15 (b). The stress on the soil element from the line load p on the surface with the width dy (Fig. 15 (c)) can be obtained as Eq. 3 by performing the integration and applying limits.

$$\sigma'_z = \frac{2p}{\pi}\frac{z^3}{(x^2+z^2)^2} = \frac{2p}{\pi}\frac{\cos^4\theta}{z} \tag{3}$$

The vertical and horizontal components of base reaction, R_V and R_H, are the sum of the three load cells measured at the base. They equal to the summation of force applied on the area of 10 cm wide and 30 cm long while the length of roller and compaction mould are 40 cm. The total number of base load cells was nine (Fig. 4 (b)).

The ratios Rv/P and R_H/P are used as dimensionless force factors. When total compaction force concentrates on the base plate, the value of Rv/P is 0.75. This value equals the ratio of loading plate length of base load cells to the length of roller (refer to Fig. 4 (b)). Defining D as the ratio between the roller distance from the center of loading plate versus the width of loading plate of base load cells, the quantity D is used as a dimensionless distance factor.

Fig. 16 shows the relationships between Rv/P and D, and curve fitting result. The curve fitting result is similar to Boussinesq's equations in shape (4^{th} layer compaction of Test No. 4). Eq. 4 shows the formula obtained from curve fitting.

$$G(x)=3/(2\pi*D^2)*1/(1+((x-C)/D)^2)^{2.5}+O \tag{4}$$

Where, D is the depth, C means the center, and O indicates the offset of fitted curve as identified in Fig. 16.

Similarly, Eq. 5 is used for shear reaction at base induced by horizontal force at the surface layer.

$$F(x)=2(x-C)^3/[\pi\cdot\{(x-C)^2+D\}^2]+O \tag{5}$$

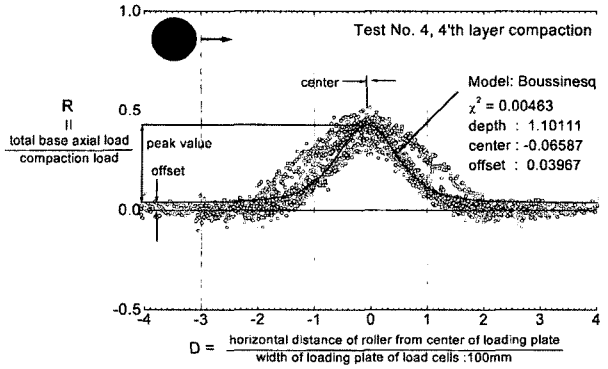

Fig. 16. Relationships between dimensionless load factor R and dimensionless distance factor D

Curve fitted data

When estimating the vertical stress of soil at any given depth, the depth z in Eq. 2 is not a variable. However, depth is used as a parameter for performing the curve fitting of measured data in this study. The obtained depth is called as the apparent depth $D_{apparent}$. The influence factor on offset is a degree of data scattering.

The main object of a curve fitting is to obtain the best values of parameter from measured data. It makes the parameters give the minimum variance of fitted curve to measured data. In this case, regression curve can be obtained.

$$\chi^2(p_1,p_2,\cdots)=\frac{1}{n^{eff}-p}\sum_i\sum_j[y_{ji}-f_j(x_{1i},x_{2i},\cdots;p_1,p_2,\cdots)]^2 \quad (6)$$

where n^{eff} is the number of measured data, p denotes the number of parameter for curve fitting, and y_{ji} represents dependent variable of measured data on independent variables such as x_{1i}, x_{2i} and x_{ji}. The difference of n^{eff} and p is defined as d, which is the degree of freedom of regression curve. A standard error was computed to evaluate the relationship between a fitted curve and measured data as follows;

$$\sigma_i=\sqrt{C_{ii}\chi^2} \quad (7)$$

where C_{ii} is a orthogonal element of variance-covariance array defined as $C=(F'\otimes F)^{-1}$. F is Jacobian array where $F_{i,j}=f(x_{1i},x_{2i},\cdots;p_1,p_2,\cdots)/p_j$. f is a fitted function for data sets of independent variable, $x_1=x_{1i}$, $x_2=x_2$.

Table 3 shows the result of stress distribution curves normalized to the width of loading plate of base load cell, 100 mm. The value of standard deviation χ^2 is less than 0.01. It can be said that the stress distribution curve can be fitted reasonably by the shape of Boussinesq's equation.

Table 3. Results of fitted stress distribution curve using Boussinesq's equation (Eq. 4.)

Test No.	Layer No.	Depth	Center	Offset	χ^2
1	1	0.798	−0.098	0	0.013
	2	0.857	−0.309	0	0.028
2	1	0.936	−0.371	0.014	0.003
	2	1.069	−0.345	0.021	0.007
	3	1.170	−0.415	0.013	0.001
	4	1.357	−0.392	0.024	0.004
3	1	0.951	−0.215	0.018	0.005
	2	0.936	−0.183	0.038	0.006
	3	0.956	−0.148	0.061	0.008
	4	1.101	−0.066	0.040	0.005
4	1	0.933	−0.354	0.027	0.003
	2	0.962	−0.239	0.029	0.008
	3	0.946	−0.245	0.049	0.007
	4	1.023	−0.190	0.041	0.006
5	1	1.011	−0.342	0.004	0.004
	2	0.962	−0.281	0.014	0.003
	3	0.988	−0.219	0.021	0.003
	4	1.138	−0.215	0.018	0.003

Vertical reaction distribution

Figs. 17 through 21 show the relationships between the dimensionless load factor Rv/P and distance factor D for

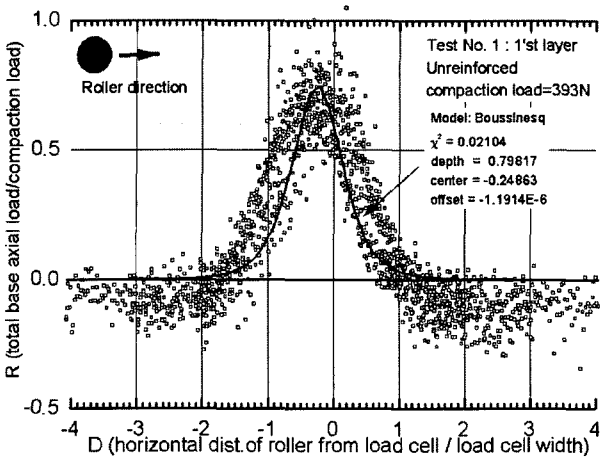

(a) 1'st layer

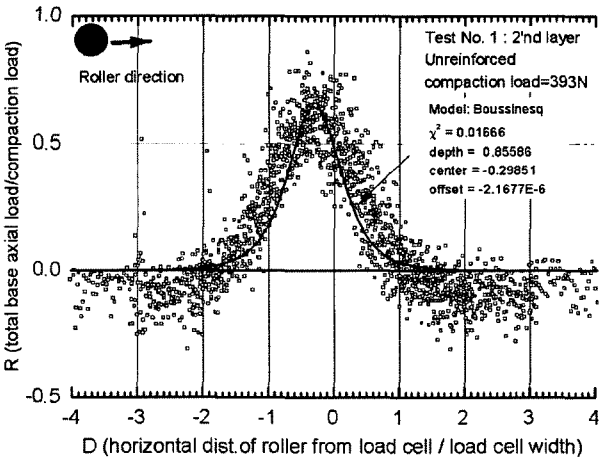

(b) 2'nd layer

Fig. 17. Relationship between R and D for Test No. 1

all tests. The discussion is focused on Test No. 2, Test No. 3, Test No. 4, and Test No. 5. Specimens for these tests have four compacted layers. The findings from these figures are:

1) The regression curves are well fitted to the data from all tests. The comparison of the behavior between each specimen was conducted with parameters from the fitted curves (Table 3).
2) The maximum vertical stress increases with the decrease of apparent depth of fitted curve. Fig. 22 shows the relationship between the number of compaction and normalized depth D_N or peak value of Rv/P. D_N is the ratio of apparent depth $D_{apparent}$ to initial thickness of soil layer H_O. It may be seen that the value of D_N decreases with the increasing number of compacted layers, while peak value of Rv/P increases. This trend is noticeable at Test No. 2 of unreinforced status. These results indicate that the compaction load is not transmitted to the base load cell effectively in unreinforced status. A possible explanation for the low stress transmission is related to the large stress distribution occurring. The contact area significantly increases by local failure below roller in Test No. 2.
3) With the reinforced specimens (Test Nos. 3, 4 and 5), the inclinations of peak value of Rv/P are greater than that of Test No. 2 as the number of compacted layer increases (Fig. 22). This behaviour may result from the following reasons; a) an increased effective confining stress zone is developed by tensile reinforcing effect below roller in which the strength of soil increases. The stress concentration effect is initiated at this zone

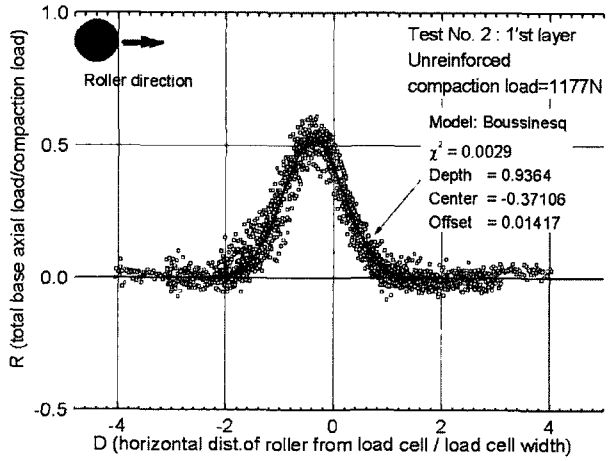

(a) 1'st layer

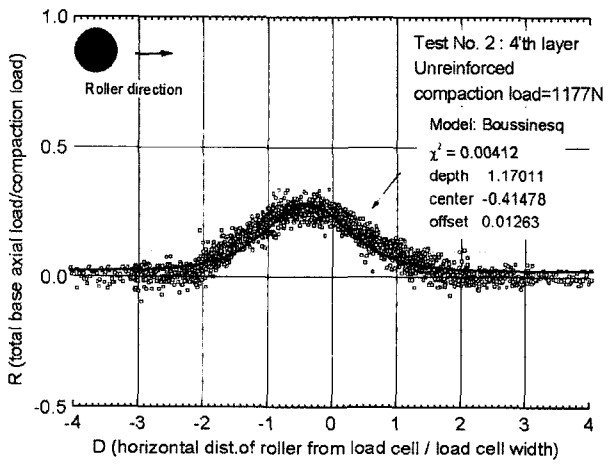

(b) 4'th layer

Fig. 18. Relationship between R and D for Test No. 2

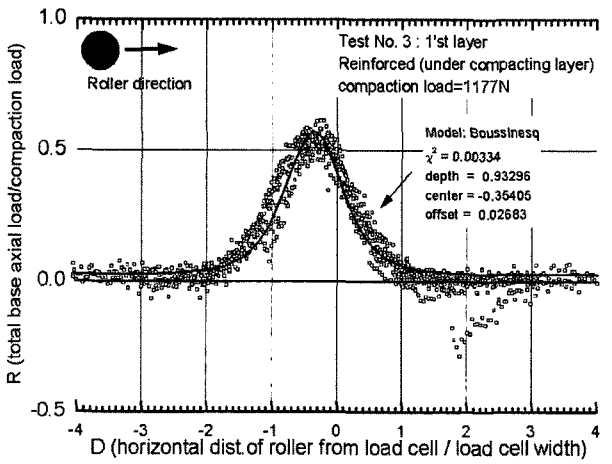

(a) 1'st layer

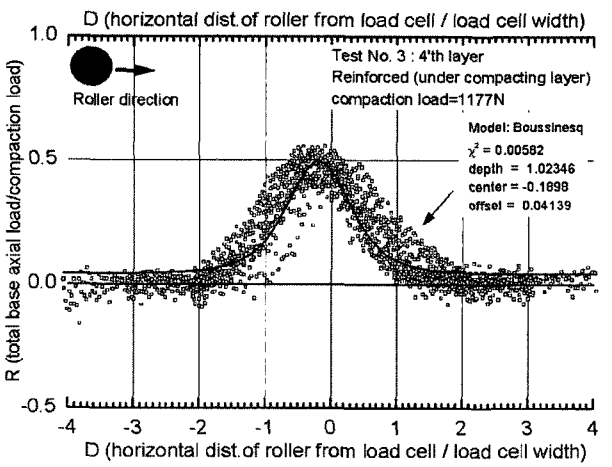

(b) 4'th layer

Fig. 19. Relationship between R and D for Test No. 3

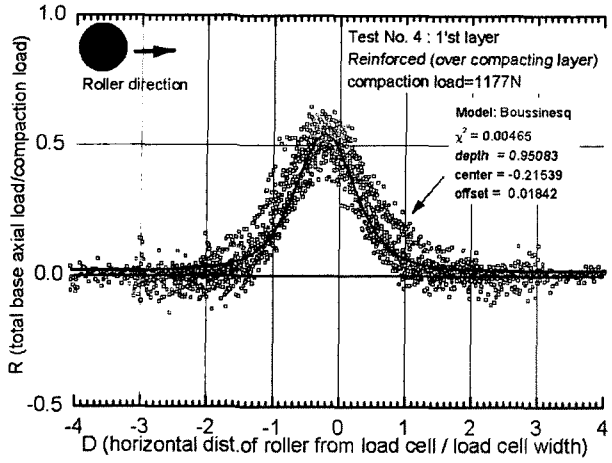

(a) 1'st layer

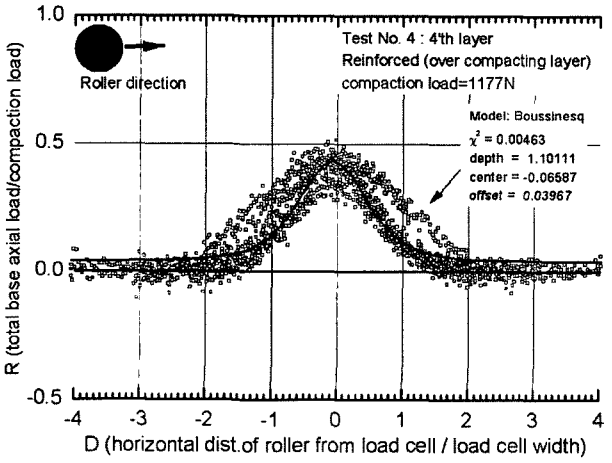

(b) 4'th layer

Fig. 20. Relationship between R and D for Test No. 4

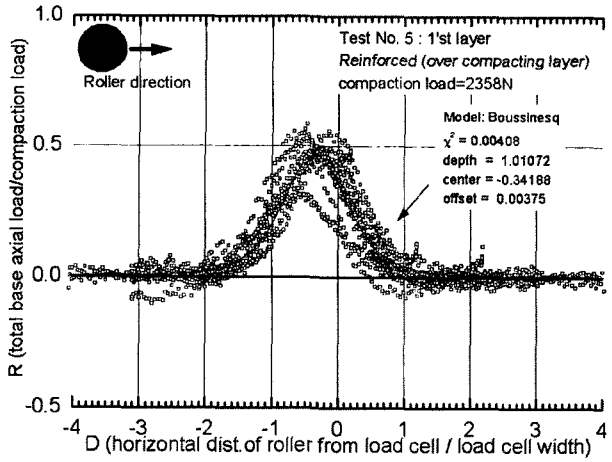

(a) 1'st layer

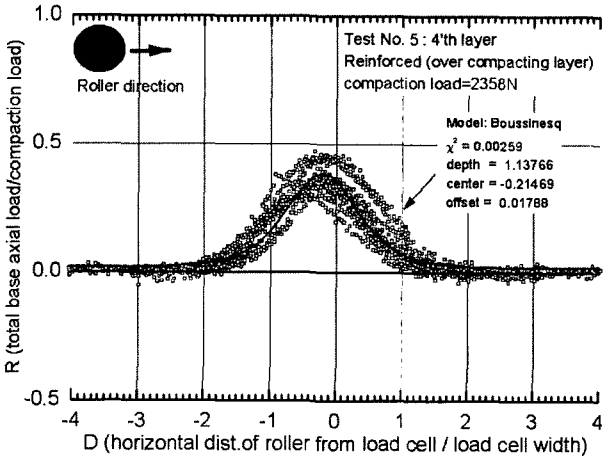

(b) 4'th layer

Fig. 21. Relationship between R and D for Test No. 5

because its stiffness is greater than that of neighbourhood soil; and b) a reinforced specimen requires smaller contact area of roller than unreinforced one to support an equivalent compaction load. The soil is well compacted by the large compaction load applied.

4) When material property of compacted soil layer is linear elastic, apparent depth should be proportional to the number of compacted layer (remember, the soil is not liner elastic material). The stress-strain property of soil will be shown more nonelastic behaviour by followings;

   a) With greater compaction load (Test Nos. 1 and 2; Test Nos. 4 and 5 in Fig. 22); Test No. 5 used twice large compaction force than that of Test No. 4. Note that the difference of D_N between Test Nos. 4 and 5 is rather small. It may happen that Test No. 5 has one more reinforcement layer than Test No. 4.

   b) With smaller depth where the stress will be evaluated;

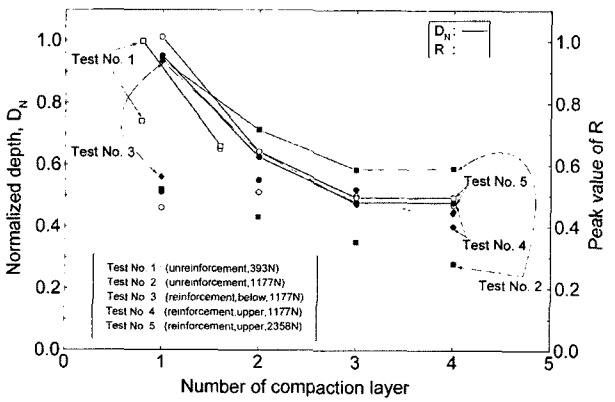

Fig. 22. Relationship between number of compaction and DN or peak value of R

The inclination of D_N increases with the increase of compacted layer. This means the increment of normalized depth, $\Delta D_N = \Delta D_{apparent} / \Delta H_O$, increases with the increase of compacted layer.

c) With smaller soil strength.
The value of D_N of unreinforced specimen is greater than that of reinforced one (refer the result of Test Nos. 2, 3 and 4 in Fig. 22).

5) For the different reinforcing method, Test Nos. 3 and 4; The main difference between Test Nos. 4 and No. 5 is that the stress distribution and increased effective confining stress are caused by surface reinforcement. The peak value of Rv/P in test No. 4 is rather smaller than that of No. 3 for 4th compacted layer. This means that the stress concentration effect is not greater than the stress distribution effect by surface reinforcement.

It can be said that compaction efficiency increases by the reinforcement due to following reasons; 1) increased effective confining stress and stress concentration, 2) decreased plastic zone of soil and increased non-homogeneous zone, and 3) increased bearing capacity of soft clay.

Effect of reinforcement on compaction

The effects of composite on mechanism of compaction could be explained as followings (Fig. 23);

1) Reinforcement effect: A greater compaction load can be applied to the reinforced specimen than unreinforced one due to the following three factors:

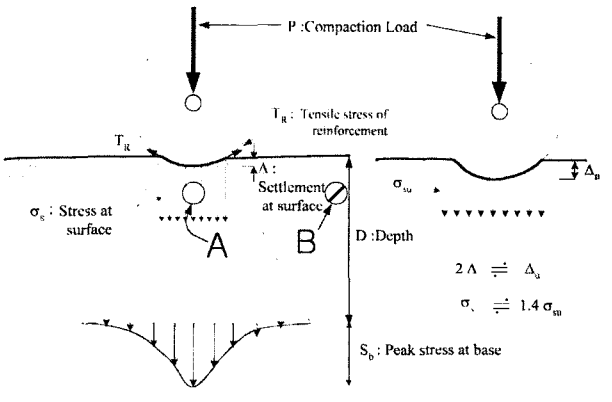

Fig. 23. Schematic diagram of stress and settlement during compaction

a) The bearing capacity of soil is increased by reinforcement. The effective confining stress of soil element increases in reinforced specimen due to tensile reinforcing effect.

b) Additional bearing capacity was achieved in the soil. The soil is well compacted because the positive excess water pressure is eliminated in specimen by drainage in reinforcement.

c) The soil stress at the surface becomes smaller due to the vertical component of tensile stress in reinforcement T_R. This means that applied load to soil can be decreased by reinforcement for the same compaction load.

2) Stress distribution effect: The stress in the ground is distributed and ratio of σ_b to σ_s decreases due to the following two factors:

a) The larger the contact area between soil and roller, the smaller the stiffness of soil. Corresponding to this, σ_s becomes smaller.

b) The value of σ_b/σ_s becomes smaller. Because the peak value of stress at base σ_b becomes smaller as the distance soil element from roller D becomes larger. This feature can be seen for unreinforced specimen as well.

3) Stress concentration effect: The ratio of σ_b to P increases due to the following two factors:

a) The transmitted stress ratio to base $R'=\sigma_b/P$ becomes larger. The contact area of soil and roller becomes smaller due to the increased bearing capacity of soil by reinforcement.

b) Soil becomes well compacted. The applied effective pressure to soil becomes larger as the degree of stress concentration becomes larger. Corresponding to this, σ_s becomes smaller.

As described above, several effects of reinforcement occurred simultaneously. The transmitted pressure to soil becomes smaller when using a reinforcement with higher stiffness. The compaction efficiency will decrease in this case. This ultimate condition may be negligible in the field condition. The stress distribution effect of reinforcement was not observed clearly in presented

result. The reinforced specimen can be compacted effectively by 1) decreased amount of pushed soil by roller, 2) increased trafficability, and 3) applied large compaction load. The main reasons are increased bearing capacity of soil and stress concentration phenomenon by reinforcement.

Location of peak stress in stress distribution curve

Fig. 23 shows the relationships between the normalized center C_N and the number of compaction for all tests. C_N means the ratio between center of fitted curve and width of base loading plate - 100 mm. The following trends can be seen from this figure:

1) A peak soil stress of the ground occurs just below the roller in static condition. However, the location of a peak stress will be changed to the front of roller due to the effect of shear force caused by moving roller in dynamic condition.
2) The applied shear force is proportional to the amount of soil thrust. Therefore the absolute value of C_N increases with a) higher compaction load, b) un-reinforced specimen than reinforced one, and c) spreaded reinforcement below the compacted layer than over.
3) The absolute value of C_N decreases by increased number of compaction layer due to increased soil depth. It can be noted that the absolute value of C_N decreases with reinforcement. This result indicates that the stiffness of reinforced soil is higher than unreinforced one.

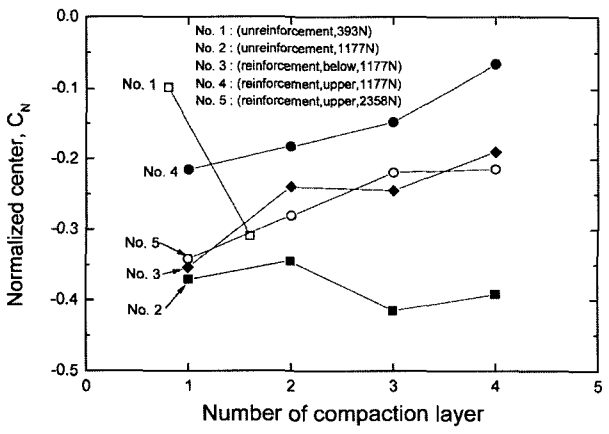

Fig. 24. Relationship between number of compaction and CN

Shear force distribution

The relationship S and D is shown in Fig 25. The fitted curves using Eq. 5 and a function of displacement used in order of nine are included in this figure. The values of center and apparent depth for the Eq. 5 are shown in Table 3. It is noted that the line of shear reaction is located before the center of roller due to load vector. The fitted curve using Eq. 5 shows relatively large difference from measured data. It results from the difference between real surface condition and horizontal surface assumptions.

Induced strain in reinforcement

Fig. 26 and Fig. 27 present the developed strain in reinforcement for Test Nos. 4 and 5 during compaction. Fig. 28 shows the maximum tensile strain in reinforcement for fourth compacted layer compaction of each test. The following trends can be seen from these figures:

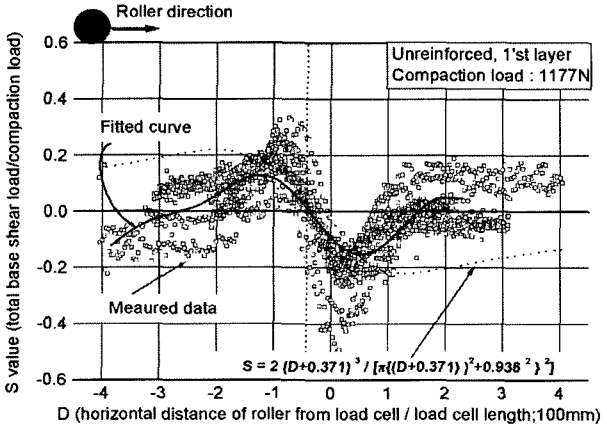

(a) 1'st layer

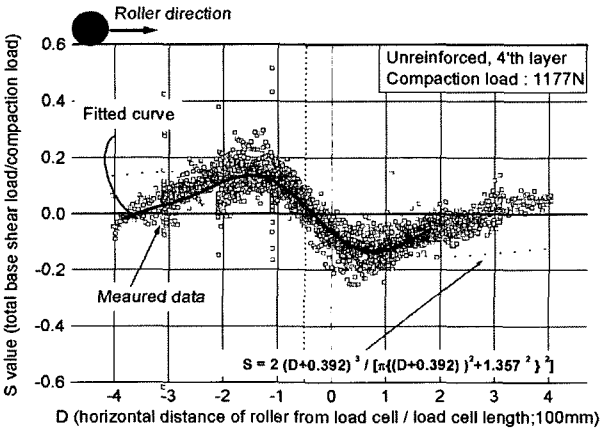

(b) 4'th layer

Fig. 25. Relationship between S and D for Test No. 1

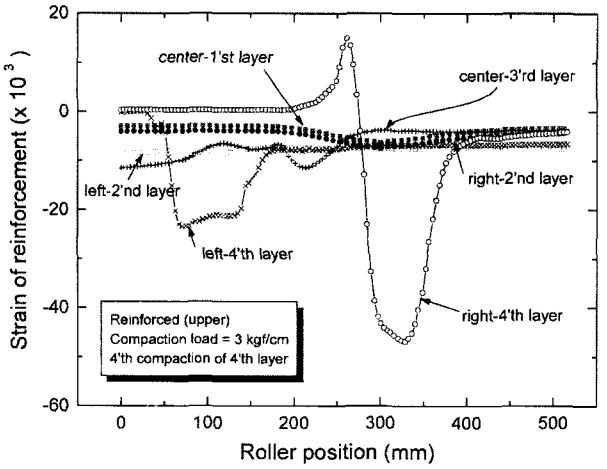

Fig. 26. Strain of reinforcement during 4'th compaction of 4'th layer (Test No. 4)

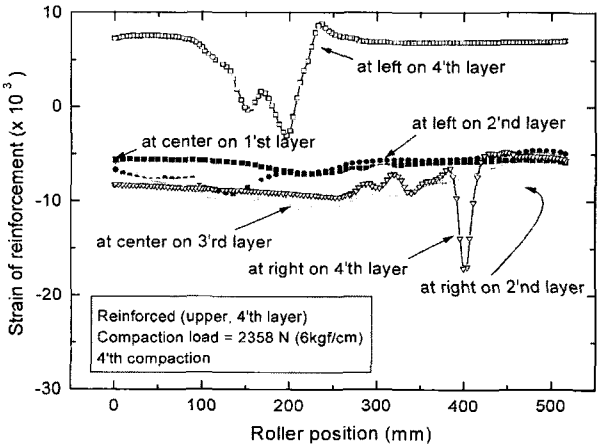

Fig. 27. Strain of reinforcement during 4'th compaction of 4'th layer (Test No. 5)

1) A reinforcement at surface was taken out to adjust thickness of compacted layer after compaction. Thus stress relaxation occurred during the reinstallation of reinforcement.
2) Two-gage electric-resistance type strain gage was used to induced strain in woven type of composite. The component could be included in measurements because strain gauges are attached to only one side of reinforcement. In spite of possible error in measurement, tensile strain certainly occurred on reinforcement during compaction.

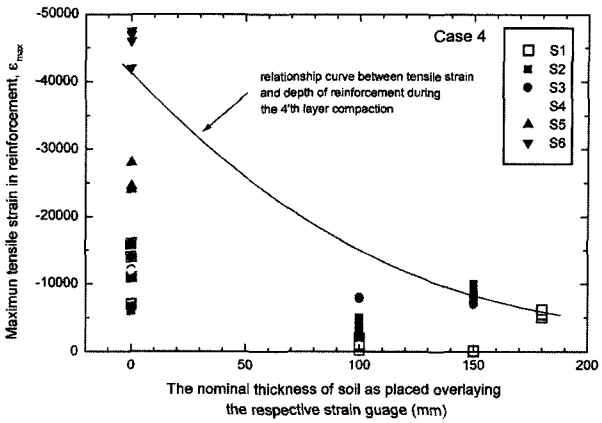

(a)

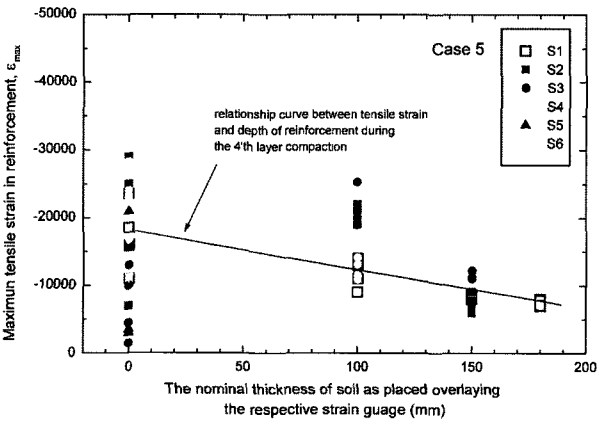

(b)

Fig. 28. Relationship between maximum strain in reinforcement and nominal thickness of soil as placed overlaying

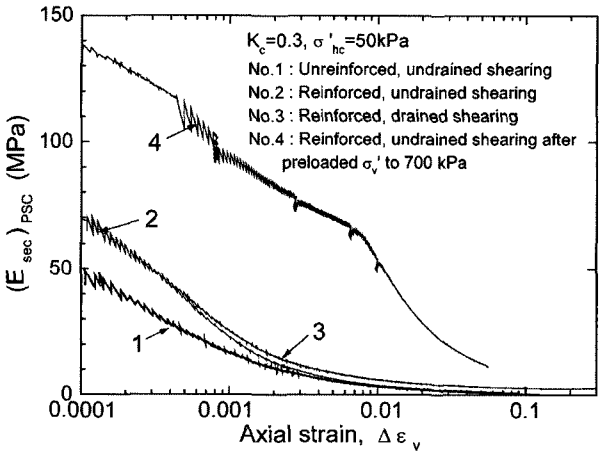

Fig. 29. Relationships between secant Young's modulus $(E_{sec})_{PSC}$ and $\log(\Delta\varepsilon_v)$ (anisotropically consolidated unreinforced and reinforced specimens)

Fig. 29 shows typical results of relationship between the secant Young's modulus.

$(E_{eq})_{PSC}$ and the $\log(\Delta\varepsilon_v)$ for unreinforced and reinforced clay. It was obtained from the plane strain test (Roh and Tatsuoka 2001). Fig. 30 presents the relationships between the equivalent Young's modulus $(E_{eq})_{PSC}$ and σ'_v. Based

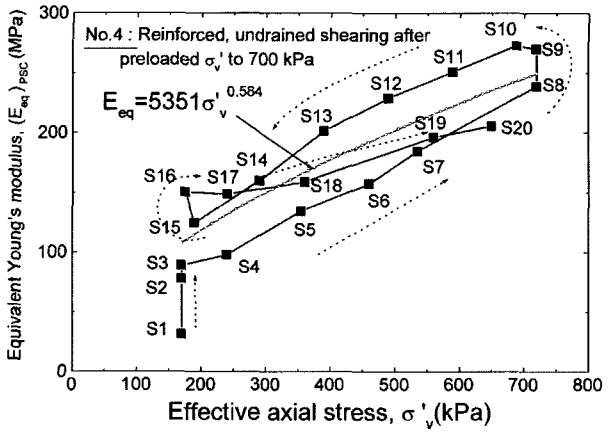

Fig. 30. Relationships between equivalent Young's modulus $(E_{eq})_{PSC}$ and σ'_v (test No. 4 on reinforced specimen)

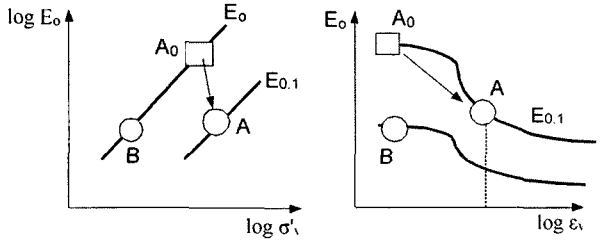

(a) Relationship between logarithmic elastic modulus and logarithmic vertical effective stress

(b) Relationship between logarithmic elastic modulus and logarithmic vertical strain

Fig. 31. Schematic diagrams of soil stiffness change during compaction

on these results, the schematic diagrams of soil stiffness change were drawn in Fig. 31 during compaction. The locations of A and B in soil are identified in Fig. 23. Ao means the initial soil state and A is the soil state at 0.1 axial strain occurring. The increased soil stiffness by reinforcement will decrease with higher strain by compaction load.

5. Conclusions

The following conclusions can be derived from the test results presented above:

(1) Without reinforcement, a large compaction load cannot be applied to the saturated soft clay due to its low shear strength and bearing capacity. If the compaction load higher than the bearing capacity of soil is applied, an embankment could fail and will not be compacted. The soil density would decreas due to the disturbance of ground by excessive compaction load.

(2) The bearing capacity of saturated soft clay increased substantially by tensile-reinforcing and drainage effect of a composite. The reinforced clay becomes well compacted by applying higher compaction load. Traffi-cability and workability can be increased by reinforce-ment. It is resulted from the fact that the ratio of shear to vertical compaction load decreased in reinforced one.

(3) Higher stress concentration occurred in the soil below roller for reinforced specimen than unreinforced one. The peak stress at base was remarkably higher in reinforced specimen than unreinforced one. A com-pacted clay layer will have high stability with high strength. One of main reasons is the positive excess pore water pressure caused by compaction decreased quickly through permeable reinforcement.

(4) The relationship between density and water content of soil follows zero-air void curve during compaction. It is due to the high water-content clay used in the present study. In the case of the greatest compaction load, the decreased amount of water content and increased dry density of soil is noticeable.

(5) The compaction efficiency is greater when the rein-forcement is located on compacted layer surface than when the reinforcement is spreaded below compacted layer. It requires reasonable evaluation method to identify the damage of reinforcement occurring during compaction.

This test result suggests that compaction efficiency can be improved for high water-contented clay backfill using tensile and drainage reinforcement.

Acknowledgements

The author deeply appreciates for the help of Prof. Tatsuoka, F, Assistant Prof. Uchimura, T. and Sugo, K., the University of Tokyo, in conducting the present study.

(received on Feb. 2, 2005, accepted on Mar. 25, 2005)